~~The~~ Relative humidity over ice as a key variable for Northern hemisphere extratropical tropopause inversion ~~layer and its correlation with relative humidity~~layers

Daniel Köhler[1,*], Philipp Reutter[1], and Peter Spichtinger[1]

[1]Institute for Atmospheric Physics, Johannes Gutenberg University Mainz, Mainz, Germany
[*]now at University of Helsinki, Helsinki, Finland

Correspondence: Philipp Reutter (preutter@uni-mainz.de)

Abstract. ~~This study investigates the influence of relative humidity with respect to ice on the extratropical~~

The tropopause inversion layer (TIL) ~~. Initially, measurements from radiosondes at a location in Germany were compared with the~~ is a prominent feature of the (extratropical) tropopause region, as it constitutes a transport barrier. Adiabatic and diabatic processes might contribute to the formation and sharpening of the inversion. For both types of processes, the relative humidity over ice is an ideal quantity for attribution; from theory and former model case studies we would expect enhanced relative humidity values in connection with a sharp TIL.

We use high resolution radiosonde data in comparison with ERA5 reanalysis data ~~from the ECMWF at the same geographic location. A high level of agreement was observed, with the expected limitation that~~ to show that there is a very good qualitative and quantitative agreement in terms of TIL features; thus, the coarser ERA5 ~~cannot resolve sharp changes in variables like humidity and stability at the tropopause as finely.~~

~~When examining the TIL with respect to mean relative humidity over ice in the upper troposphere,~~ data can be used for further investigations. In a second step, we investigate the the connection between TIL features and relative humidity measures in both, radiosonde and ERA5 data; here, a clear relationship ~~with stability~~ becomes evident. Moister profiles, on average, exhibit significantly higher maximum values of the Brunt-Väisälä frequency N^2, indicating a more stable stratification of the tropopause in these cases. This result holds true in both radiosonde measurements and ERA5 data. Considering the thickness of the TIL layer, an inverse pattern emerges. In this case, moister and more stable TILs exhibit a lower thickness.

~~The strong agreement between radiosondes~~ Because of the good agreement between radiosonde and ERA5 ~~allows for geographical and seasonal analyses using~~ data, we extent the investigation using solely ERA5 data ~~alone~~for seasonal and regional investigations. These analyses reveal consistent relationships in various extratropical regions of the Northern Hemisphere under different meteorological conditions. Differences in the strength of the dependence of TIL properties on relative humidity over ice are evident.

1 Introduction

~~The Earth'~~

The Earth's atmosphere, a dynamic and complex multiscale system, plays a pivotal role in regulating our planet~~'~~'s climate and weather patterns. Within this intricate atmospheric structure lies the troposphere, the layer closest to the Earth~~'~~'s surface and the site of most of our planet~~'~~'s weather phenomena. At its upper boundary to the adjacent stratosphere, the static stability is highly increasing until reaching stratospheric values. This transition layer of increasing stability is often called tropopause region, with more or less strict definitions (see, e.g., **?**). About 20 years ago, **?** were able to demonstrate with high-resolution radiosonde data that sometimes the troposphere encounters a ~~distinct and intriguing feature~~ strong temperature inversion known as the tropopause inversion layer (TIL). ~~**?** introduced the investigation of the TIL using high-resolution radiosonde profiles. Their approach involved employing a tropopause-centered averaging method, where they utilized~~ This feature is most prominent, if the vertical coordinate system is transformed into a system utilizing the thermal tropopause as the reference point for the vertical coordinate instead of sea level. Sometimes, averaging methods are additionally used to demonstrate the main features on a larger vertical scale.

Situated at the interface between the troposphere and the stratosphere, the TIL represents a unique and enigmatic region characterized by an abrupt increase in temperature with altitude — a significant departure from the typical decrease in temperature observed throughout the lower atmosphere. Thus, a sharp TIL constitutes a strong transport barrier for trace gases~~and other inert substances.~~ , cloud particles, and other key variables like vertical motion. Beyond this the importance of the TIL also lies within the diagnostics of upper troposphere and lower stratosphere (UTLS) structures.

Since its discovery, a couple of ~~hypothesis~~ hypotheses were developed to explain the origin and formation of the TIL. **?** showed in model ~~analysis~~ analyses that baroclinic waves lead to a net sharpening of the tropopause, which leads to ~~stronger TIL. More precisely, an anticyclonic circulation produces~~ a stronger TIL~~, whereas a cyclonic circulation tends to decrease the strength of the TIL.~~ . **?** and **?** provided further evidence to support the impact of baroclinic waves on the TIL. Additionally, **?** suggested a radiative forcing mechanism, where the interaction of ozone and water vapour with radiation are contributing to the TIL formation and persistence. ~~The calculations of **?** and the observations of **?** suggest that the radiative forcing mechanism is a dominant effect for the formation and evolution of the TIL .~~

~~To investigate the latter mechanism further, we examine the correlation between the relative humidity~~ In a recent model study, **?** were able to show that the formation of the TIL is probably driven by a combination of different adiabatic and diabatic processes. In a first step, evolving baroclinic instabilities lead to a compression of isentropes, which in turn results into sharper gradients of the stability. Relevant processes in this respect are horizontal convergence in anticyclonic regions, strong upward motions, e.g. triggered by convective instabilities, and gravity waves triggered by the large scale flow, respectively. Since these changes are mostly adiabatic and thus reversible in general, in a second step diabatic processes as turbulence/mixing, cloud formation and resulting latent heat release and radiative heating/cooling by trace gases (as water vapor) modify the TIL irreversible. As showed by **?**, the diagnostics of these processes is quite difficult and from measurements it might be quite impossible to disentangle the contributions of the different processes.

However, by careful inspection of the scenario, there is a quantity, which might be considered as a proxy for these different processes. The relative humidity (with respect to a stable phase of water, i.e., liquid or solid) is the control variable for many cloud processes. On the other hand, this variable, as combined by the mass concentration of water vapor, pressure, and temperature, is a good indicator for adiabatic expansion processes (i.e. cooling); high values of RH can be expected if moist air is adiabatically lifted. In the tropopause region within the low temperature regime (i.e. $T < 235\,\mathrm{K}$), relative humidity over ice (RHi) ~~, a measure for water vapor in the UTLS region, and the TIL. For this purpose,~~ is the relevant quantity, since solid ice is the stable phase there. Thus, RHi might be a good indicator for the strong lifting of air masses in baroclinic instabilities, thus working as a proxy for strong TILs.

Water vapor is a strong greenhouse gas, especially in the infrared range; the absolute concentration of water molecules controls the amount of emission and absorption. Particularly in case of a moist layer we would expect a strong emission of energy in the infrared spectrum, and thus a cooling of the layer. However, the total amount of water molecules is not the only reason for strong emissions. Since the atmosphere is layered, the concentration of water vapor in adjacent layers is also of importance. If the layers of different temperatures have a similar amount of water vapor, the emitted radiation is easily absorbed by the layers on top. Thus, a strong gradient in concentration (e.g. a layer with low concentration on top of a layer with high concentration) leads to a much stronger cooling rate than in a situation with weak gradients. Since it is difficult to measure (or determine) the gradient in water vapor concentrations, a good compromise is the use of relative humidity. Since it is linear in the water vapor concentration, it represents the gradients in a meaningful way. Because of small temperature changes in adjacent layers with strong vapor gradients, the impact of the temperature is quite negligible. For the tropopause region, this phenomenon was investigated in a study by **?**; a stronger gradient in RHi leads to a much more pronounced cooling on top of the moist layer.

In summary, the use of relative humidity over ice in the tropopause region might help to detect strong TILs. Or in other words, correlations between high values of RHi and strong TILs would corroborate the two step formation of TILs with adiabatic and diabatic components. Therefore the use of RHi is highly relevant for the investigation of the tropopause inversion layer.

The aim of this study is twofold: First, we want to demonstrate that even with the coarse resolution of ERA5 data it is possible to represent features in the tropopause region as the tropopause inversion layer (TIL) in a qualitative way. In addition, the quantitative analysis shows that the absolute values of the TIL properties as, e.g., maximum values of static stability quite closely agree with the values as obtained from high resolution data (i.e. radiosondes). Second, we want to investigate the correlation of the quantity of relative humidity with the strength of the TIL. Because of the general formation mechanisms of the TIL in terms of adiabatic (dynamic) and diabatic processes, the quantity relative humidity is the relevant variable, which is related to the formation processes of the TIL. In this study, we make the first attempt to evaluate reanalysis data on a statistical basis, generalizing the findings from case studies and idealized simulations as carried out by **?**.

For the first investigation, nearly 10,000 high-resolution radiosonde ascents from a weather station in Germany (Idar-Oberstein) are analyzed. Additionally, this investigation is combined with the ERA5 reanalysis data from the European Centre for Medium-Range Weather Forecasts (ECMWF) for the same location. This approach allows for an evaluation of the quality of ERA5 data concerning the TIL at the presented ~~German~~ location. Given that the TIL is associated with strong gradients in stability, the comparison of model data with high-resolution measurements is indispensable.

In the second step, we investigate the correlation between relative humidity and static stability from the ERA5 data in order to corroborate the findings of **?** in a statistical way. Upon successful assessment of data quality, we can extend our analysis to examine the TIL in a similar manner at other locations. We have focused on regions at a similar geographical latitude but with varying frequencies of baroclinic activity. This approach enables us not only to unravel seasonal differences but also to incorporate the influence of atmospheric or even regional peculiarities into the interpretation of the results.

This study is organized as follows. In Section 2 we present details on the data and methods used to identify the important quantities of TIL characteristics. Section 3 presents the results. First a comparison of measurements and reanalysis data is provided, followed by an investigation of the influence of the relative humidity on TIL properties. Finally, we extend the examination on geographical and seasonal variations. Conclusions are found in section 4.

2 Data and Methods

In this section we describe the data sets, the relevant variables, and the methods for the statistical investigations.

2.1 Data

This study is partly based on radiosonde data from a measurement site at Idar-Oberstein (Germany, 49.69° N, 7.33° E). This site was selected, because the German weather service (Deutscher Wetterdienst, DWD) provides 9 years of high resolution ~~radiosondes~~ radiosonde data as open access. The exact used time frame spans from the 1st of January 2011 to the 31th of December 2019.

The radiosonde measurements are compared with the reanalysis data set ERA5 (**?**) provided by the ECMWF. After the comparison and evaluation of the data at the selected site, profiles at different geographical locations are investigated based on the ERA5 data set.

2.1.1 Radiosonde data

Idar-Oberstein is one out of 12 stations in Germany, where the DWD executes synoptic (daily at 00, 06, 12, 18 UTC) high resolution ~~radiosondes~~ radiosonde soundings. The station is located at 49.69° N and 7.33° E at 376 m altitude above sea level.

For the radiosonde measurements the Vaisala RS92-SGP (01/01/2011 - 12/03/2017 & 15/06/2017 - 31/12/2019) sonde and the Vaisala RS41-SGP (28/03/2017 - 14/06/2017) sonde are used, respectively. The characteristics of the two types of radiosondes are very similar; however, the RS41-SGP has a slightly higher precision than the RS92-SGB (**?**). Therefore, the data is treated as if the entire data set is measured by the RS92-SGP radiosonde.

During one ascent of the radiosonde, the meteorological variables are measured with a time resolution of 0.5 Hertz, providing the longitude ~~&~~ and latitude by a GPS-sensor, the geopotential height ~~Φ_g (m)~~Φ_g [m], the ambient pressure ~~p (hPa)~~p [hPa], the temperature ~~T (K)~~ T [K] and the relative humidity over liquid water ~~RH (%)~~RH [%], respectively. In a first approximation geopotential height Φ_g is equal to the vertical height z. For the considered data set this approximation is quite good, because of Idar-Oberstein's latitude of 49.69° N and ~~the altitude of the measurements never exceed 20 km.~~our focus on investigations in the UTLS.

This investigation ~~focus~~ focuses on the upper troposphere and lower stratosphere (UTLS). For obtaining a complete and consistent data set, profiles with a maximum height lower than 20 km and profiles containing missing data are discarded. Over the period from 01/01/2011 to 31/12/2019, the data set contains 10224 single profiles. 419 profiles are discarded, 311 due to insufficient maximum height, 19 due to missing data and 89 due to ~~unscientific temperature (> 500 K)~~ unreliable values of temperature and relative humidity~~(> 300 %)~~.

The uncertainties of the RS92-SGP regarding the measurements are given by the manufacturer (?). The temperature sensor has a reaction time less than ~~2.5 seconds~~ 2.5 s and a total uncertainty of ~~0.5° C~~0.5 °C. The humidity sensor has a response time between ~~0.5 s and 20 s~~ 0.5 s and 20 s with a total uncertainty of RH = 5 %. The pressure sensor has a total uncertainty of ~~1 hPa~~ 1 hPa for 1080 to ~~100 hPa and 0.6 hPa~~ 100 hPa and 0.6 hPa for 100 to ~~3 hPa~~3 hPa.

The radiosonde humidity data are time-lag corrected according to **?** and the water vapor measurements are corrected using the algorithm and coefficients used by **?**. Although the algorithm was developed for the RS92 sonde, it can be applied to the few data points as obtained from the RS41-SGP sonde.

2.1.2 ERA5

ERA5 is the ~~latest~~ most recent reanalysis product of the ECMWF (**?**). The reanalysis is a mix of a ~~past model forecast~~ recalculation of past weather with one fixed forecast model version (IFS CY41R2) and assimilated measurements made ~~at the forecast~~ for each available time. The high resolution data set has a horizontal resolution 0.25° in longitude and latitude. The vertical dimension of the atmosphere is ~~calculated on~~ represented by hybrid sigma/pressure (model) levels in ERA5 (**?**), the number of levels is 137 of which only levels up to the lower stratosphere are used. In the tropopause region, the vertical resolution is about 300 m.

For the comparison with the radiosonde data we obtained pseudo-radiosonde profiles, i.e. a vertical column at ~~the~~ a fixed grid point. The vertical ~~column~~ profile is extracted at the ~~closest grid point of the model to 49.75° N and 7.25° E, which will be compared to the radiosondes data set.~~ grid point 49.75° N and 7.25° E, which is the closest grid point of ERA5 to the actual location of Idar-Oberstein (49.69° N and 7.33° E). The date and the time of the extracted columns are matched with the reduced ~~radiosondes~~ radiosonde data set to obtain a maximum of comparability between the data set. For comparison, the relevant variables, as, e.g., the geopotential height ~~Φ_p~~ Φ_g are calculated.

2.1.3 Data gridding

In order to guarantee comparability between the ~~data sets~~ radiosonde data and ERA5 it is mandatory to grid ~~the data sets~~ them vertically. A regular grid leads to a ~~consistent~~ evenly spacing between data points, which in in turns allows for a ~~improved~~ straightforward statistical analysis. The base of the regular grid is the geometric height z.

Radiosondes use the buoyancy force to ascend, thus the vertical speed and consequently the vertical resolution is not constant. The buoyancy speed of the used radiosondes is ranging from ~~$2\,\mathrm{ms^{-1}}$ to $8\,\mathrm{ms^{-1}}$~~$2\,\mathrm{m\,s^{-1}}$ to $8\,\mathrm{m\,s^{-1}}$ (with a mean around $5\,\mathrm{m\,s^{-1}}$), returning a vertical resolution of 4 to ~~16 m, respectively~~16 m, respectively, what is usually recognized as high-resolution data (**?**). The final data grid has a ~~30 m~~ 30 m resolution starting from station height ~~376 m~~ 376 m above sea level up to ~~20 km~~ 20 m in order to reduce the amount of unused data. The interpolation is performed with a cubic spline, which offers sufficient accuracy for this study.

~~The model levels change height with the given atmospheric state, so the geopotential height grid of~~ By converting the ERA5 ~~is irregular and inconsistent with respect to time . The data sets~~ data from a pressure grid to a grid with the geometric height z, the latter grid changes from one point in time to the next with each atmospheric state. Thus, the ERA5 data set is interpolated on the same grid as the radiosondes data (~~376 m to 20 km, with 30 m~~ 376 m to 20 km, with 30 m resolution) using a cubic spline. The ERA5 data set is heavily over-sampled with a ~~30 m~~ 30 m resolution, meaning the high resolution does not provide additional information~~, but~~ ; however, the choice is made in order to make the ERA5 data set comparable to the radiosonde data. Finally, we obtained comparable data sets.

2.2 ~~Methods~~Relevant variables

Since most of the desired variables are not directly available, they are calculated from the available ~~information.~~ variables in the data set. Therefore, the calculation of the relative humidity with respect to ice RHi (%), the potential temperature θ (K) and the Brunt-Väisälä-frequency N^2 (s^{-2}) are described below.

~~We choose the variable RHi as a measure for humidity, since this is the thermodynamic control variable for many ice cloud processes, i.e. determining nucleation, growth and evaporation of ice crystals. In addition this humidity variable is a linear variable (in the range between 0 and about 170%), which makes the evaluations simpler and more robust, than using the specific humidity, which in turn does not allow a relation to cloud processes without additional variables. The choice of RHi as a variable is related to the low temperature regime in the UTLS ($T < 240$ K) with hexagonal ice as a stable phase of water.~~

2.2.1 ~~Calculation of essential variables~~

~~The~~ The relative humidity is defined as the ratio of the partial pressure of water vapour p_v over the saturation pressure p_s~~.~~ ~~The saturation pressure is dependent on the phase, i.e. p_s is different between the liquid /gas-boundary compared to the ice/gas-boundary~~, which depends on the relevant stable phase (liquid or solid water phase). In this study, the parameterization described by **?** is used for the saturation pressure with respect to liquid water $p_{s,liq}$ and ice $p_{s,ice}$. This choice is motivated by the fact that these formulae are used for radiosonde evaluations ~~.~~ by default. The use of RHi as a variable is related to the low temperature regime in the UTLS (for $T < 240$ K, see, e.g., **?**) with hexagonal ice as a stable phase of water.

The quantity RHi is derived from RH (relative humidity over liquid water) of the radiosonde using the following relationship:

$$RHi = RH \cdot \frac{p_{s,liq}(T)}{p_{s,ice}(T)} \tag{1}$$

Note, that the most accurate and physically sound formulations for the saturation pressure (over ice or liquid) according to **?** deviate only slightly from the formulae above in the respective temperature regime, leading to a positive bias in the resulting relative humidity over ice of a few percent, which increases with decreasing temperatures. However, for ~~our investigations the~~

~~deviation is negligible. The quantity~~ temperatures at the extratropical tropopause region, this deviation does not crucially affect the investigations.

The variable RHi ~~is derived from RH of the radiosonde using the following relationship:~~ constitute not only a measure for atmospheric humidity, but also serve as a good proxy for determining the relevant processes, which lead to the formation and further strengthening of the TIL: Adiabatic cooling leads to higher values of RHi, and diabatic processes as cloud formation and radiative feedbacks are also controlled by this quantity. In addition this humidity variable is a linear variable (in the range between 0 and about 170%), which makes the evaluations simpler and more robust, than using the specific humidity, which in turn does not allow a relation to cloud processes without additional variables.

$$\cancel{RHi = RH \cdot \frac{p_{s,liq}}{p_{s,ice}}}$$

The ERA5 data set provides the humidity as the specific humidity q (~~kg kg^{-1}~~ kg kg^{-1}) which is converted to the relative humidity over ice using the following approximation:

$$\mathrm{RHi} \approx \cancel{\frac{q \cdot p}{\epsilon \cdot p_{s,ice}}} \frac{q \cdot p}{\epsilon \cdot p_{s,ice}(T)} \tag{2}$$

with the ratio of the molar masses of water and air, $\epsilon = \frac{M_{\text{mol,water}}}{M_{\text{mol,air}}} \approx 0.622$.

Potential temperature θ is ~~a quantity in atmospheric sciences, which is~~ equivalent to the specific entropy of dry air, assuming the ideal gas approximation ~~. This quantity~~ for dry air. It allows to compare parcels of air at different pressures levels, and, by definition, it is a conserved quantity for isentropic (i.e. adiabatic) processes. We use the common definition of θ as stated in eq. (**??**) with a constant specific heat capacity ~~$c_p = 1.005\,\mathrm{kJ\,kg^{-1}\,K^{-1}}$~~ $c_p = 1.005\,\mathrm{kJ\,kg^{-1}\,K^{-1}}$ of dry air:

$$\theta = T \left(\frac{p_0}{p}\right)^{\kappa} \text{ with } \kappa = \frac{R}{c_p} \approx \frac{2}{7} \tag{3}$$

Here, $p_0 = 1000$ hPa denotes the reference pressure level, and ~~$R = 287.05\,\mathrm{J\,kg^{-1}\,K^{-1}}$~~ $R = 287.05\,\mathrm{J\,kg^{-1}\,K^{-1}}$ is the specific gas constant for air. This definition with constant c_p is accurate enough for investigations in the ~~UTLS~~ tropopause region (see discussion in **?**). The relation to specific entropy of dry air is given by $\mathrm{d}s = c_p \mathrm{d}\log(\theta)$.

The static stability ~~or~~ of dry air or, more commonly, the Brunt-Väisälä-frequency squared N^2 is a common measure for the stability of the dry atmosphere (**?**). $N^2 < 0$ characterises an unstable stratification, $N^2 = 0$ a neutral stratification and $N^2 > 0$ a stable stratification, respectively. The free troposphere is dominantly stable and the stratosphere is considerably more stable than the troposphere. The static stability is derived from the buoyancy force (i.e. Archimedes' principle) and can be approximate by:

$$N^2 = \frac{g}{\theta} \cdot \frac{\partial \theta}{\partial z} = \frac{g}{T}(\Gamma_d - \Gamma) \tag{4}$$

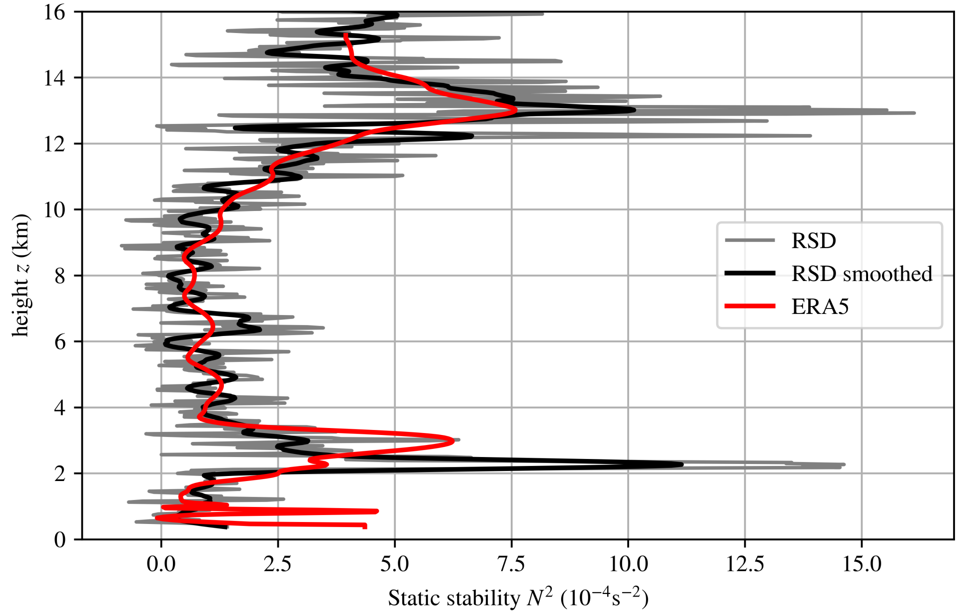

Figure 1. Example of a static stability profile from the 02.01.2011 0 UTC with (grey) the calculated N^2 from radiosonde data, (black) the ~~330 m~~ 330 m window smoothed N^2 from radiosonde data and (red) the calculated N^2 from ERA5 data.

with ~~$g = 9.8066\,\mathrm{m\,s^{-2}}$~~ $g = 9.8066\,\mathrm{m\,s^{-2}}$ the (mean) gravitational acceleration, ~~Γ_d~~ $\Gamma_d = \frac{g}{c_p}$ the dry adiabatic lapse rate, and $\Gamma = \frac{\partial T}{\partial z}$ the actual temperature lapse rate based on the geometric height z, respectively.

This approximation is working under the assumption of dry air and returns on average too high values for the Brunt-Väisälä-frequency~~(?). It is nonetheless used~~; moisture leads to strong decrease in the static stability, even if no phase change is triggered (?). However, a moist, and commonly accepted, analog to dry static stability is still missing, although there are some attempts for a consistent treatment (?). Therefore we use dry static stability to ensure comparable results with literature which use the dry approximation ~~(????)~~(e.g. **????**).

As the measurements of a ~~radiosondes~~ radiosonde are discrete, a numerical approximation of the derivative is necessary. Since the grid increments are quite small, the numerically derived gradients are highly variable. Thus, a centered approximation of the 4^{th} order is used ~~:~~

$$\frac{\partial \theta}{\partial z} \approx \frac{4}{3}\frac{\theta_{z+1} - \theta_{z-1}}{z_{z+1} - z_{z-1}} - \frac{1}{3}\frac{\theta_{z+2} - \theta_{z-2}}{z_{z+2} - z_{z-2}} \tag{5}$$

in order to smooth the resulting finite gradient approximations. However, even this high order method leads to a highly variable N^2 profile. For a better handling, the profile is additionally smoothed using a running mean with a window of 330 ~~m~~m, as can be seen in Fig. **??**.

2.2.1 ~~Calculation of tropopause characteristics~~

2.3 Calculation of tropopause characteristics

2.3.1 ~~Tropopause height~~Definition of tropopause

The tropopause separates the troposphere and the ~~lower stratosphere~~stratosphere, constituting a transport barrier for trace gases and cloud particles. There are several attempts to define the tropopause using different approaches. We list the most common approaches; however, afterwards we will use the classical definition of a thermal tropopause, as defined by the World Meteorological Organisation (WMO) in the middle of the last century. More details about the history and difficult definition of the tropopause we refer to the studies by **???** and **?**.

The tropopause can be defined on the basis of different variables, as e.g., physical temperature, potential temperature, potential vorticity (PV), or even chemical trace gases, as e.g. ozone. In the classical definition by the WMO (1957) the lapse rate of the temperature is taken into account. The full criterion can be stated as *"The first tropopause is defined as the lowest level at which the lapse rate decreases to 2 K per kilometer or less, provided also the average lapse rate between this level and all higher levels within 2 kilometers does not exceed 2 K"* (**?**). For the tropics, sometimes the so-called cold point temperature is used, i.e. the first minimum in the free troposphere of the physical temperature (**?**).

In a further step, the potential temperature θ can be used as a basis variable. The gradient of θ can be used as a simple measure for the static stability, thus influencing tracer transport (see, e.g., **?**). The tropopause can be defined as the height level at which a certain threshold in the gradient $\frac{\partial\theta}{\partial z}$ exceeds a certain threshold (e.g. $\frac{\partial\theta}{\partial z}\big|_{\mathrm{thres}} \sim 0.012\,\mathrm{K\,m^{-1}}$, see **?**). Following the discussion by **?**, it seems that a refined version of this definition might be most robust. From the potential temperature, the Brunt-Väisälä (or buoyancy) frequency can be calculated, see eq. (**??**). Instead of using the Brunt-Väisälä frequency itself, **?** introduced the level of the maximum gradient of N^2 as the tropopause; actually, this is the level of the maximum curvature of the temperature, which can be set in relation to the residual circulation.

From an atmospheric dynamics perspective, the potential vorticity as an adiabatic invariant is investigated. The level of a certain (but kind of arbitrary) threshold is the set as dynamical tropopause. While often the threshold of 2 PVU is used, **?** showed that the value in terms of transport barriers can vary between 1.5 and ~~is characterised by an inversion of the temperature gradient. One important criterion~~ 5 PVU, also depending on the season. The threshold of 3.5 PVU often produces a dynamical tropopause height, which is close to the thermal tropopause level as derived by WMO criterion (**?**).

Finally, chemical trace gases are used to define the ~~(thermal)tropopause is the WMO (World Meteorological Organisation) criterion: *"The first tropopause is defined as the lowest level at which the lapse rate decreases to 2 K per kilometer or less, provided also the average lapse rate between this level and all higher levels within 2 kilometers does not exceed 2 K"* (**?**). Note, that this definition is based on a consideration of large/synoptic scale variations, assuming~~ tropopause as a transport layer. Actually, from this point of view the tropopause is not an ideal clear defined interface between troposphere and stratosphere, but merely a transition layer (see, e.g., discussion in **?**). The depth of the transition layer was investigated using tracer-tracer correlation, e.g. using ozone and carbon monoxide (**?**). Since there is a clear signal in the ozone concentration in the different vertical layers (troposphere vs. stratosphere), a threshold criterion might be used to define the ozonopause, which should be close to tropopause levels derived from other definitions. **?** used a threshold of ozone mixing ratio in order of 100-110 ppb and showed that the ozonopause is usually quite close to the thermal tropopause. This approach was used further for a simple discrimination of aircraft data (see, e.g., **?**) and for other applications without using a full 3D data set of meteorological variables. In some investigations, the hygropause (i.e. the minimum in water vapor concentrations) was also used as a proxy. However, this approach is not really successfully applied for data analysis. Although there might be more modern definitions of the tropopause level, we stick with the classical definition by **?**. This is mostly due to a better comparison with former studies on the tropopause inversion layer (e.g. **??**); however, this definition represents the nature of the transport barrier very well and is still a standard definition for the daily reports of all weather services in the world.

One should keep in mind that almost all definitions of the tropopause level were driven by the large scale perspective of atmospheric dynamics, i.e. using the viewpoint that the vertical change in the thermodynamic variables (i.e. temperature and pressure, respectively) is smooth enough. ~~However, this is not the case for investigations of~~ This viewpoint is clearly represented in the WMO definition using lapse rates, where changes over a long vertical extent are investigated. In general, this definition requires a certain vertical resolution, whereas deviations in both directions might raise issues. For very coarse resolution data as in low resolution radiosonde reports, former reanalysis data or climate models, the determination of lapse rates causes problems, which can be handled with some refined methods (see, e.g., **??**).

For high resolution data, as ~~radiosondes or~~ in operational radiosondes or partly in the new generation of reanalysis data (see, e.g., a similar discussion about front detection in **?**)~~. However, for consistency with former investigations, we adopt this criterion and incorporate this in an algorithm to determine the tropopause height TP_z in both data sets. There are other definitions of~~, the variables are not smooth enough for the determination of gradients; actually, the high resolution leads to strong variations or even nonphysical noise. In extreme cases, the WMO criterion is never fulfilled, since the lapse rate is crucially changing within the required extension of $2\,\mathrm{km}$, see also discussion in **?**. For high resolution data, averaging (e.g. running means) of high resolution data or higher order finite difference methods for determining the gradients can be applied, see, e.g., the calculation of $\frac{\partial\theta}{\partial z}$ in eq. (**??**). However, the ~~tropopause (e.g.using the potential vorticity for a dynamical tropopause, or the ozone profile for a chemical tropopause); however, for a better comparison with former investigations (e.g. **??**) we use the thermal tropopause , which represents the transport barrier very well. For investigations of the different tropopause definitions we refer to **?**.~~ question remains if the definition of a tropopause layer as driven by the large scale viewpoint of atmospheric dynamicists is still meaningful, if we consider much smaller scales. At least for investigations of convective events, some effort is made to find more robust measures for the tropopause characteristics (see, e.g., **?**).

~~A tropopause relative height framework is implemented. We~~

2.3.2 Relative coordinates

In order to be able to compare the large number of radisonde data and ERA5 profiles, a tropopause-centered coordinate system was introduced. For this purpose, the thermal tropopause is identified in each radiosonde and ERA5 profile for Idar-Oberstein and defined as the tropopause height TP_z. This means that all profiles now live in the same coordinate system and can be

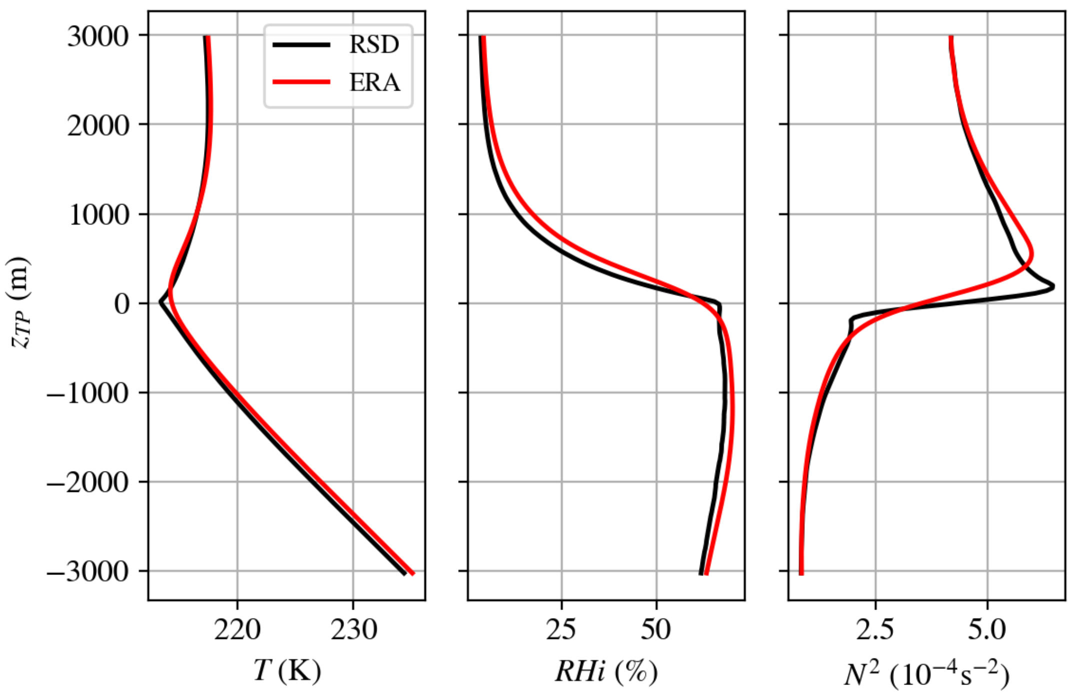

Figure 2. The average vertical profile in the tropopause relative height z_{TP} coordinate system of temperature T, relative humidity over ice RHi and static stability N^2 for the radiosondes (black) and ERA5 (red).

averaged to obtain mean profiles of temperature, humidity and static stability. Therefore, we introduce a new height variable

$$z_{TP} = z - TP_z \tag{6}$$

relative to the tropopause height TP_z (as derived by the WMO criterion, see above). Negative altitude values z_{TP} denote the upper troposphere, whereas positive altitude values z_{TP} represent the lower stratosphere. For the averaging process the single profiles are transformed into the z_{TP} coordinate system and the arithmetic mean of a meteorological variable $\chi \in \{$temperature, relative humidity, static stability$\}$ is calculated, summing over all profiles at a certain height.

The mean profiles relative to tropopause height of temperature, static stability (N^2), and RHi can be seen in Figure **??** for the radiosonde measurements (black) and the corresponding ERA5 data set (red) at the location of Idar-Oberstein. Even for the mean profiles the characteristics of the TIL, i.e., the strong increase in N^2 at around TP_z can be seen clearly, as described in the next section. However, Figure **??** also shows that the results differ between radiosonde and reanalysis data. In the temperature profile of ERA5, the minimum temperature is less pronounced, as well as the values in RHi at the tropopause level. The static stability profile shows a deviation of the maximum in N^2, i.e. the level of the maximum is shifted towards higher altitudes and the maximum is less pronounced as compared to the high resolution radiosonde data. These differences are mainly based on

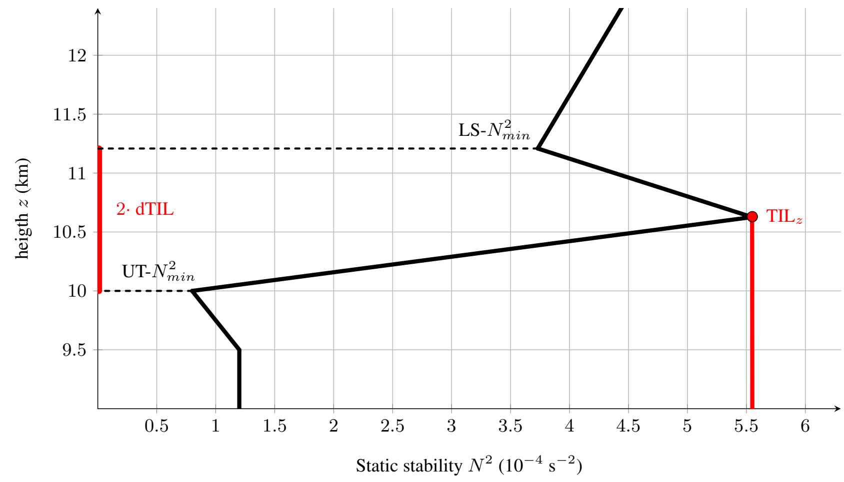

Figure 3. A schematic drawing of the different diagnostics of the tropopause inversion layer, i.e. the TIL depth dTIL and the strength of the TIL, sTIL, respectively. These features (minima and maximum in N^2) can also be seen in the realistic profile represented in figure **??**.

the vertical resolution of the data sets, which is significantly lower in the case of the ERA5 data than in the radiosonde data. As a result, sharp gradients cannot be resolved as good, as can be seen in particular when looking at N^2. A detailed comparison between the radiosonde and ERA5 data can be found in Section **??**.

2.3.3 Tropopause inversion layer

~~Another important measure in the~~ The tropopause ~~region is the tropopause~~ inversion layer (TIL) ~~. The TIL~~ is a region of extraordinary high static stability within the tropopause region and was found by averaging vertical profiles with respect to the tropopause level. The TIL is also present in single vertical profiles of radiosondes (**?**) and models (**?**). The ~~importance of the TIL lies within the diagnostics of~~ high stability in the TIL region represents a barrier to vertical motion (**?**) and is therefore important for understanding the composition of the air in the upper troposphere and lower stratosphere~~(UTLS) structures and as a transport barrier for vertical motion (?).~~

. Although there are investigations of the TIL properties since more than two decades, a clear (or even common) definition of the TIL and its main features (as e.g. strength) is missing. For this study, we define the TIL strength ~~sTIL~~ **sTIL** as the maximum of the static stability N^2_{max} within ~~3 km~~ 3 km above tropopause level and the altitude level of N^2_{max} as the TIL height TIL$_z$. Two additional heights are defined through two minimum values of N^2: UT-N^2_{min} is the height of the minimum of N^2 in the upper troposphere, and LS-N^2_{min} is the height of the minimum of N^2 within ~~5 km~~ 5 km above TIL height. The TIL depth ~~dTIL~~ **dTIL** is half of the height difference between the UT-N^2_{min} and LS-N^2_{min}. The ~~diagnostic~~ diagnostics of the TIL with the main features and the newly introduced quantities sTIL and dTIL are summarized in Figure **??**.

~~In the radiosonde data, the features~~ If one of the features such as UT-N^2_{min} or LS-N^2_{min} could not be determined~~in~~ , these profiles were excluded from consideration in this study. This affected 126 profiles, ~~which were subsequently discarded as a~~

~~result. Therefore, the final data set was reduced to~~ so that in the end 9678 ~~profiles~~ profiles were included in the analysis in this study. Note, that the real profile of high resolution ~~radiosonde measurements.~~ data (radiosonde and ERA5) as represented in Figure **??** includes all the features of the scheme shown in Figure **??** (UT minimum of N^2, maximum of N^2, LS minimum of N^2). After averaging over many tropopause-centered profiles, some features might be lost in the mean profiles (e.g. Figure **??**), although they are still visible in the single profiles – otherwise the profiles would be discharged in the analysis.

2.3.4 Calculation of humidity measure

The analysis of the humidity of the upper troposphere and the lower stratosphere is based on the average humidity with respect to ice below the TIL, denoted by wRHi. It is calculated by averaging RHi from the height of the ~~500 hPa pressure surface~~ ~~$p500_z$~~ $500\,\mathrm{hPa}$ pressure surface z_{p500} up to the TIL level TIL_z, as defined in (**??**).

$$\mathrm{wRHi} = \cancel{\frac{1}{\mathrm{TIL_z} - p500_z}}\frac{1}{\mathrm{TIL_z} - z_{p500}} \int_{\cancel{p500_z}\, z_{p500}}^{\mathrm{TIL_z}} \mathrm{RHi}(z)\,dz \approx \cancel{\frac{1}{\mathrm{TIL_z} - p500_z}}\frac{1}{\mathrm{TIL_z} - z_{p500}} \sum_{\cancel{z=p500_z}\, z=z_{p500}}^{\mathrm{TIL_z}} \mathrm{RHi(z)}\,\Delta z \quad (7)$$

This moisture (or humidity) ~~measure~~ is used in the further course to sort the vertical profiles according to different moisture contents. ~~This quantity is quite robust due to small scale variations, thus representing the overall impact of humidity on the TIL.~~

3 Results

Based on the spatially and temporally highly resolved ERA5 data, the properties of the tropopause region related to the static stability and relative humidity in this region are investigated in more detail. ~~In a first step, the~~ As stated in the motivation, our goal of this study is twofold. First, we want to show that there is good agreement of high resolution radiosondes and ERA5 data in terms of representing the main features of TILs in the extratropics. Therefore, the measured data of the radiosondes are compared with the corresponding data of the reanalysis model. ~~Afterwards, the correlations between moisture and the TIL properties are examined~~ Second, we want to show that relative humidity is the key quantity for TILs, thus there is a strong correlation between high humidity measures and sharp/strong TILs. This is investigated in more detail, also with the consideration of seasonal and geographical differences.

3.1 TIL properties in measurements and reanalysis data

A very good agreement between the radiosonde measurements and the reanalysis data is the basic prerequisite for further investigations based on the ERA5 data. Therefore, in a first step, the deviations between radiosonde measurements and reanalysis data for the variables temperature T, relative humidity with respect to ice RHi and static stability N^2 are investigated. In the next step, the results for the different heights (TP_z, TIL_z) are investigated. Finally, the TIL properties such as TIL thickness and TIL depth are compared.

3.1.1 Comparision of temperature, relative humidity with respect to ice

The deviation between radiosonde measurements and ERA5 data in a variable χ are quantified by the average measure ~~$\overline{D}(\chi)$~~ $\overline{D}_{\mathrm{abs}}(\chi)$ for every single profile. This quantity can be calculated as follows:

$$\overline{D}_{\mathrm{abs}}(\chi) := \frac{1}{z'-z_0}\int_{z_0}^{z'} \cancel{E(\chi)-R(\chi)\mathrm{d}}|E(\chi)-R(\chi)|\mathrm{d}z \approx \frac{1}{z'-z_0}\sum_{z_0}^{z'} \cancel{E(\chi(z))-R(\chi(z))}|E(\chi(z))-R(\chi(z))|\Delta z \tag{8}$$

with z_0 the start and z' the end height of the averaging, χ the meteorological variable of interest, E, the ERA5 profile and R the radionsonde profile, respectively. Δz is the height difference between two adjacent levels. We chose a metric including absolute values of differences in order to avoid undesired cancellation effects of positive and negative contributions. In this sense, we used a metric inspired by the L_1-norm. Thus, the resulting distributions are expected to be skew and might have (exponential) decaying tails. The resulting data set is visualised in a probability bar chart and the corresponding median, mean and standard deviation for the different variables are presented in figures **??**, **??**, and **??**, respectively.

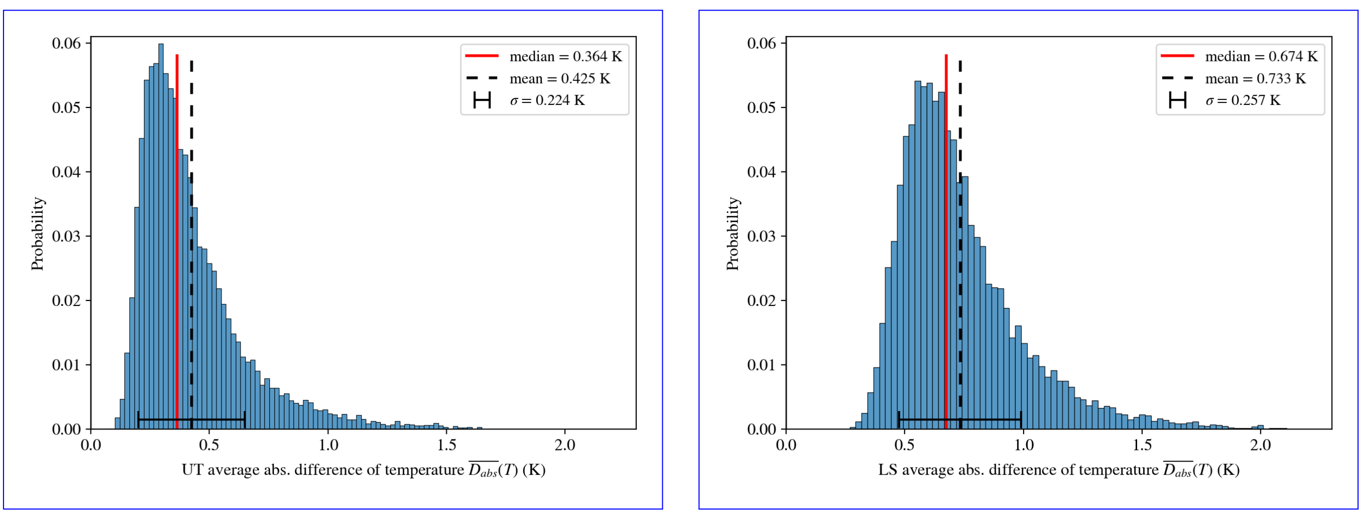

(a) Upper troposphere UT

(b) Lower stratosphere LS

Figure 4. Probability distribution of average difference of temperature $\overline{D}(T)$ between ERA5 and radiosondes for upper troposphere UT (a) and the lower stratosphere LS (b). The median is displayed in red, the mean is represented by a dashed black line and standard deviation σ is represented as error bar. ~~The zero line is denoted as a gray thin line. Positive values mean that ERA5 is warmer than the radiosonde.~~

The temperature deviations between the radiosondes and ERA5 for the upper troposphere ($z_0 = -3000\,\mathrm{m}$, $z' = 0\,\mathrm{m}$, Fig. **??**) show a ~~Gaussian distribution~~ skew distribution with a median of ~~0.027 K and~~ 0.37 K, a mean of ~~0.034 K indicating a~~

~~near symmetric distribution. The mean and median being positive show that the ERA5 reanalysis is slightly warmer than the radiosonde measurements.~~ $0.43\,\mathrm{K}$ and a standard deviation $\sigma = 0.22\,\mathrm{K}$. For the lower stratosphere ($z_0 = 0\,\mathrm{m}$, $z' = 3000\,\mathrm{m}$) the distribution of the temperature deviation is similar (**??**). However, the median (~~0.130 K~~$0.67\,\mathrm{K}$) and mean (~~0.121 K~~$0.73\,\mathrm{K}$) values are significantly larger~~. The positive sign again means~~, with a standard deviation of $\sigma = 0.26\,\mathrm{K}$. Generally we know that ERA5 has on average slightly warmer temperatures compared to the measurements. In order to ~~interepret~~ interpret these results, it should be mentioned that the measurements have an uncertainty of $0.5\,\mathrm{K}$ according to the manufacturer (**?**).

For deriving a robust statement about the humidity impact on the TIL in the tropopause region, the relative humidity with respect to ice (RHi) is used. As mentioned above, this is the key thermodynamic control variable for ice cloud processes, thus determining also the life cycle of ice clouds. The consistency of the moisture data ~~are~~ is also important for the description of the average relative humidity with respect to ice wRHi. The distributions in Figure **??** for mean ~~difference~~ differences show a shift to higher ~~values~~ deviations of RHi in ERA5. This behavior is due to the fact that ERA5 data does not capture the moisture ~~gradient~~ gradients at the tropopause as sharply as the radiosonde ~~. In other words, in a thin layer above the tropopause, RHi decreases much faster in the radiosonde data compared to ERA5.~~ data. The humidity features, i.e. the fine structures, are smeared out; this is partly due to the coarse vertical resolution of the ERA5 data but probably also due to issues in the data assimilation of moisture in cold temperature regimes. This difference dominates the value of $\cancel{\overline{D}(\chi)}$ $\overline{D}_{\mathrm{abs}}(\chi)$ for each individual vertical profile~~. The differences are distributed near symmetrically centered around 1.249 %~~; thus, we would expect less steep gradients for RHi in the ERA5 data. These differences are again distributed with some skewness, leading to quite similar median value ($12.95\,\%$) and mean value ($13.99\,\%$) in the upper troposphere~~and 1.230 %~~, and accordingly to median value ($2.96\,\%$) and mean value ($3.56\,\%$) in the lower stratosphere. The standard deviation for the upper troposphere is ~~$\sigma = 10.318$ %~~$\sigma = 6.57\,\%$ which is a considerable deviation, where relative humidity over ice ranges from 0% - 105%. In the lower stratosphere, where relative humidity is generally much lower than in the troposphere, the standard deviation is ~~$\sigma = 2.831$ %~~$\sigma = 2.49\,\%$.

The static stability or Brunt-Väisälä-frequency squared N^2 represents the main ~~criteria~~ criterion to identify the tropopause inversion layer and its characteristics. Looking at the probability distribution (Fig. **??**), there exists a notable difference between the upper troposphere and the lower stratosphere. In the upper troposphere (Fig. **??**), ERA5 has a tendency to be more stable with a mean = ~~$0.068 \cdot 10^{-4}\,\mathrm{s}^{-2}$~~$0.40 \times 10^{-4}\,\mathrm{s}^{-2}$and a median = ~~$0.058 \cdot 10^{-4}\,\mathrm{s}^{-2}$~~$0.43 \times 10^{-4}\,\mathrm{s}^{-2}$. The distribution is skewed towards smaller average difference values of N^2 ~~. The majority of the differences lie in the $(0.068 \pm 0.102) \cdot 10^{-4}\,\mathrm{s}^{-2}$ interval.~~ with a standard deviation of $\sigma = 0.15 \times 10^{-4}\,\mathrm{s}^{-2}$ When comparing the average differences and the standard deviation of N^2 to the static stability for the upper troposphere ~~$N^2 = 1.2 \cdot 10^{-4}\,\mathrm{s}^{-2}$~~$1.2 \times 10^{-4}\,\mathrm{s}^{-2}$ (**?**), the static stability is represented well in the ERA5 reanalysis.

In the lower stratosphere (Fig. **??**), ERA5 is ~~more unstable~~ less stable compared to the radiosonde data with a mean = ~~$-0.055 \cdot 10^{-4}\,\mathrm{s}^{-2}$~~1.0 and a median = ~~$-0.046 \cdot 10^{-4}\,\mathrm{s}^{-2}$~~$1.07 \times 10^{-4}\,\mathrm{s}^{-2}$ with tendency to smaller absolute values of static stability~~.~~; the standard deviation is $\sigma = 0.31 \times 10^{-4}\,\mathrm{s}^{-2}$

The reason for the lower stability in the lower stratosphere in ERA5 is the tropopause inversion layer, which arises through a strong gradient of potential temperature. Due to the lower vertical resolution of ERA5, strong gradients in the variables are less pronounced, leading smaller values of static stability thus resulting in a ~~too unstable~~ less stable vertical profile in the lower

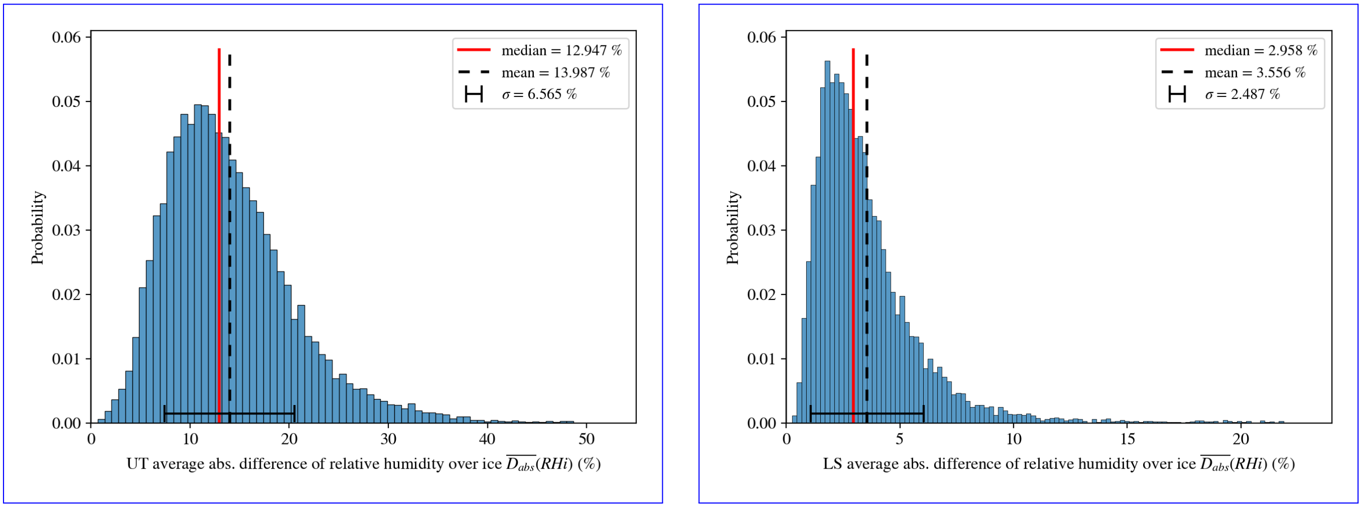

(a) Upper troposphere UT

(b) Lower stratosphere LS

Figure 5. Probability distribution of average difference of relative humidity over ice $\overline{D}(\mathrm{RHi})$ between ERA5 and radiosondes for upper troposphere UT (a) and the lower stratosphere LS. With the median in red, the mean in dashed black and standard deviation σ as error bar. ~~The zero line is denoted as a gray thin line. While the mean difference is small, the spread in the deviation is quite large~~

stratosphere. Nonetheless, the average difference of ~~$0.055 \cdot 10^{-4}\,\mathrm{s}^{-2}$~~ $\sim 10^{-4}\,\mathrm{s}^{-2}$ is small compared to the average value of N^2 of ~~$4.0 \cdot 10^{-4}\,\mathrm{s}^{-2}$~~ $4 \times 10^{-4}\,\mathrm{s}^{-2}$.

Overall, we can state that the quantitative agreement between the high resolution radiosonde data and the ERA5 data is high enough to represent the profiles of T, RHi, and N^2 in a satisfying way. However, the more important issue in the comparison is the qualitative representation of TIL features in both data sets, as will be investigated in the next section.

3.2 TIL properties and humidity

In the following sections we investigate the relationship between TIL properties and moisture, especially in terms of TIL strength and thickness. As a measure for humidity we use the averaged relative humidity with respect to ice (wRHi) as introduced earlier in equation **??**.

3.2.1 TIL strength and humidity

First, we classify the vertical profiles into tropopause inversion layers of different strengths (sTIL). The classification of sTIL is based on three classes~~: lowsTIL (sTIL $< 6.8 \cdot 10^{-4}\,\mathrm{s}^{-2}$ for the radiosondes, sTIL $< 5.2 \cdot 10^{-4}\,\mathrm{s}^{-2}$ for~~, i.e. low, medium, and high values of sTIL, with different intervals for the radiosonde data and the ERA5 ~~), mediumsTIL ($6.8 \cdot 10^{-4}\,\mathrm{s}^{-2} <$ sTIL $< 11.2 \cdot 10^{-4}\,\mathrm{s}^{-}$ for the radiosondes, $5.2 \cdot 10^{-4}\,\mathrm{s}^{-2} <$ sTIL $< 8.4 \cdot 10^{-4}\,\mathrm{s}^{-2}$ for ERA5) and high sTIL ($11.2 \cdot 10^{-4}\,\mathrm{s}^{-2} <$ sTIL for the radiosondes, $8.4 \cdot 10^{-4}\,\mathrm{s}^{-2} <$ sTIL for ERA5). The~~ data, respectively. The ranges are represented in Table **??**. The classification criteria

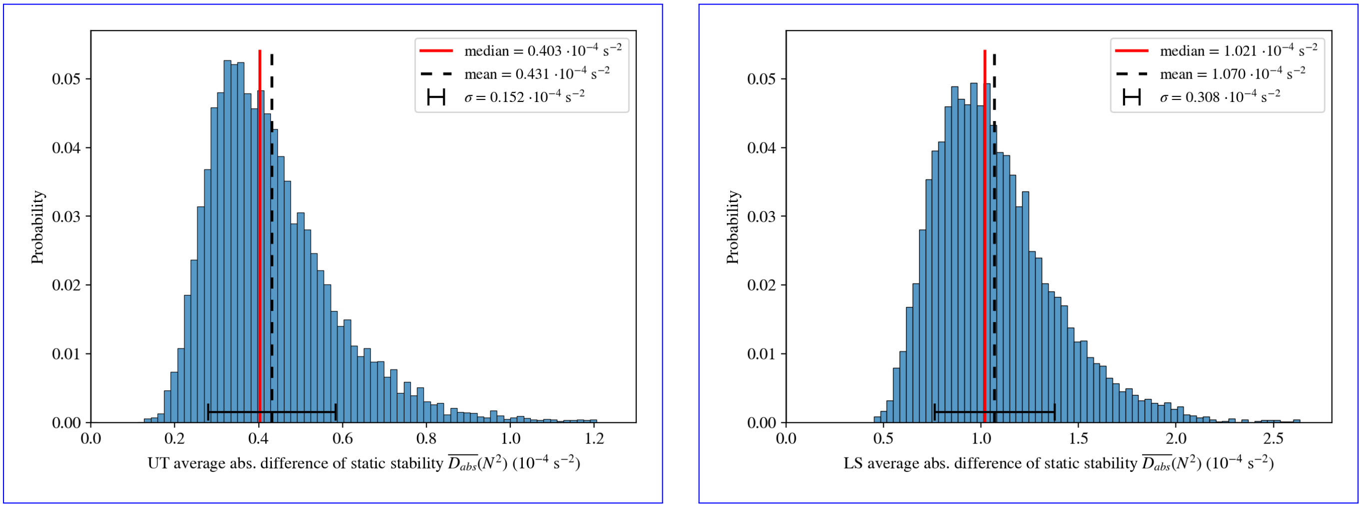

(a) Upper troposphere UT

(b) Lower stratosphere LS

Figure 6. Probability distribution of average difference of static stability $\overline{D}(N^2)$ between ERA5 and radiosondes for upper troposphere UT (a) and the lower stratosphere LS. With the median in red, the mean in dashed black and standard deviation σ as error bar. ~~The zero line is denoted as a gray thin line. The UT is more stable in ERA5 as compared to the radiosonde data, whereas in the LS the ERA5 data indicates smaller values (lower stability) than the radiosonde data.~~

Table 1. Values of sTIL for the three different classes (low/medium/high) in the radiosonde data set and the ERA5 data set

sTIL	low	medium	high
RS	$< 6.8 \times 10^{-4}\,\mathrm{s}^{-2}$	$[6.8 \times 10^{-4}\,\mathrm{s}^{-2}, 11.2 \times 10^{-4}\,\mathrm{s}^{-2}]$	$> 11.2 \times 10^{-4}\,\mathrm{s}^{-2}$
ERA5	$< 5.2 \times 10^{-4}\,\mathrm{s}^{-2}$	$[5.2 \times 10^{-4}\,\mathrm{s}^{-2}, 8.4 \times 10^{-4}\,\mathrm{s}^{-2}]$	$> 8.4 \times 10^{-4}\,\mathrm{s}^{-2}$

were chosen such that one third of the vertical profiles fall into each category (low, medium, high). Since the distributions of metrics between ERA5 and radiosondes differ, the exact values of the classification boundaries are also different. Figure **??** shows the corresponding mean profiles for temperature, RHi, and static stability for the radiosondes (left) and the reanalysis data (right).

As expected the ERA5 reanalysis is not able to capture the sharp gradients as well as the high resolution radiosondes. This is noticeable with the sharp kinks in temperature T and relative humidity with respect to ice RHi at tropopause level (z_{TP} = 0 m) and the sharp spikes in the static stability N^2, which are present in the radiosonde data, but are smoothed out in the ERA5 data. Despite of these issues related to the resolution of ERA5, the reanalysis data show the same qualitative behaviour for temperature and RHi, respectively. Thus, the ERA5 data set can be used consistently for the investigation of TIL in the extratropics.

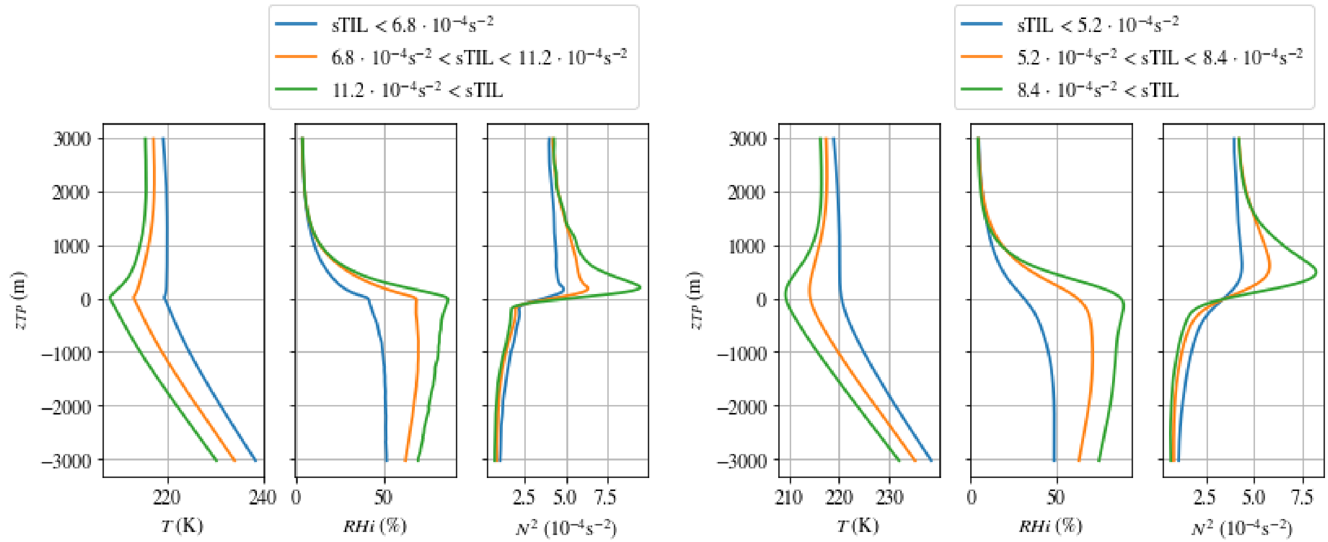

(a) Radiosondes (b) ERA5

Figure 7. The mean vertical profiles for radiosondes RSD (a) and ERA5 (b) of temperature T, relative humidity over ice RHi and static stability N^2 in the tropopause relative height z_{TP}. The mean profiles are classified in terms of tropopause inversion layer strength sTIL. Colors indicate the different sTIL categories. blue: low sTIL value category, orange: medium sTIL value category, green: high sTIL value category. The exact boundary values of the categories are found in the respective legend.

With the focus on the temperature profile, stronger TILs seem to be correlated with colder temperatures and thus possibly with higher tropopause heights. However, this interpretation is somewhat problematic, since warmer and colder profiles with higher and lower tropopause heights are compared. Some altitude shifts in the profiles might weakening or even cancel out these effects. The correlation between a sharper temperature inversion above the tropopause and a stronger TIL is certainly expected, because the TIL strength is derived ~~from the static stability N^2 which is dependent of the potential temperature gradient and thus the temperature gradients (eq. **??**& **??**~~directly from the temperature gradients (Eq. **??**).

~~Changing the focus to the correlations of RHi~~Thus, we shift our investigations to the connection between relative humidity and TIL strength. Here, we find ~~that the TIL is stronger for higher RHi values appearing in the upper tropopause ($z_{TP} < 0$ m) and right above the tropopause (0 m < z_{TP} < 500 m). In the low sTIL category, the average RHi equals~~ two robust features, which can be clearly seen in the different classes of the TIL strength sTIL. For the class with the highest sTIL values (green line in Figure. **??**) we find enhanced values of RHi throughout the troposphere until the tropopause level; here, the averaged values of RHi are usually above 70%. For the medium class, the relative humidity values show averaged values of about 60%, whereas in the low sTIL class, the relative humidity values are around 50%~~and is almost constant in the upper tropopause. The medium sTIL category is correlated with an average RHi above 60 % with a slight increase towards the tropopause. The high sTIL category shows average RHi above 70 % with a steep increase towards the tropopause. The increase in relative humidity~~

Table 2. Maxima in N^2 for the different classes of wRHi as represented in figure **??**

N^2_{max}	low wRHi	medium wRHi	high wRHi
RS	$7.3\times10^{-4}\,\mathrm{s}^{-2}$	$8.2\times10^{-4}\,\mathrm{s}^{-2}$	$9.3\times10^{-4}\,\mathrm{s}^{-2}$
ERA5	$5.7\times10^{-4}\,\mathrm{s}^{-2}$	$6.5\times10^{-4}\,\mathrm{s}^{-2}$	$7.0\times10^{-4}\,\mathrm{s}^{-2}$

~~with respect to ice with increasing height up to the tropopause is a potential indication that vertical motion in the atmosphere is correlated as well to stronger TILs (?), since the resulting adiabatic cooling of air would in turn lead to an increase in RHi~~.

~~As expected the~~ The signal is the same for radiosonde data and ERA5 ~~reanalysis is not able to capture the sharp gradients as well as the high resolution radiosondes. This is noticeable with the sharp kinks in temperature T and relative humidity with respect to ice RHi at tropopause level(z_{TP} = 0 m) and the sharp spikes in the static stability N^2, which are present in the radiosonde data, but are smoothed out in the ERA5 data. Despite of these issues related to the resolution of ERA5, the reanalysis data show~~ data, with slight changes in the values.

In addition, we find that for the high sTIL class the RHi gradient on top of the moist layer is much sharper than for the other two classes. Again, we see a clear decrease in the RHi gradient for the medium and low sTIL classes, respectively.

In summary, we find a sharper or stronger TIL for

1. higher RHI values in the troposphere, and
2. sharper gradients in RHi on top of the moist layer (at the tropopause height and above).

The first feature of enhanced RHi values (with a slight increase with height towards the tropopause level) can be interpreted as a signal of the adiabatic processes (e.g. during baroclinic instability evolution) enforcing a vertical upward motion (with compressing isentropes) and thus an increase in RHi. A higher value of RHi might also indicate a stronger (or even longer) adiabatic process. The second feature of a strong moisture gradient at the tropopause level might point to diabatic processes leading to irreversible foramtion of the ~~same qualitative behaviour for temperature and RHi, respectively~~TIL. Actually, **?** could show that the strongest radiative cooling in moist tropopause layers was triggered for strong RHi gradients. Thus, the ~~ERA5 data set can be used consistently for the investigation of TIL in the extratropics~~variable RHi points to both processes according to higher values and steeper gradients, respectively.

Another way to investigate the relationship between humidity and TIL strength is to look at the sTIL distribution as a function of the mean RHi. For this purpose, the sTIL data of the radiosondes and of ERA5 were divided into three RHi classes: low wRHi (wRHi $\leq$ 45 %), medium wRHi (45 % < wRHi $\leq$ 70 %) and high wRHi (70 % <wRHi), respectively. These distributions are represented in Fig. **??**, for radiosonde data (left panel) and ERA5 data (right panel), respectively.

We find in Fig. **??** that the probability density function (PDF) of the TIL strength is correlated with higher values of ~~wRHi of~~ averaged relative humidity with respect to ice (wRHi). This is deducible by the shift of the PDF curve to higher sTIL values with higher wRHi categories. This shift is most obvious at the position of the maximum of the mode of the PDF~~. The mode for~~

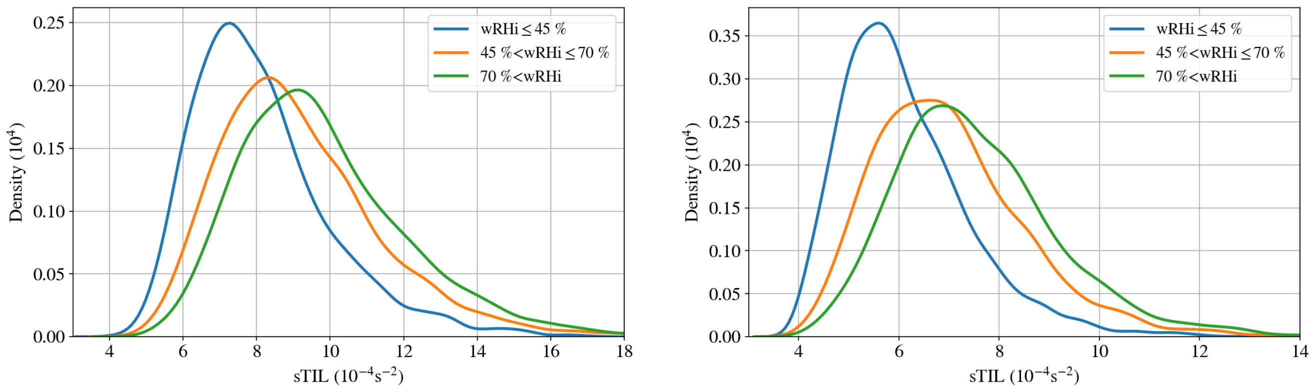

(a) radiosondes (b) ERA5

Figure 8. The probability density function for the radiosondes RSD (a) and ERA5 (b) of the TIL strength sTIL for categories of the average relative humidity over ice wRHi. Colors indicate the different categories with respect to wRHi. blue: low category (wRHi $\leq$ 45 %), orange: medium category (45 % < wRHi $\leq$ 70 %), green: high category (70 % < wRHi). Note the slightly different scale in the sTIL axis in both parts

~~the radiosondes shifts from a maximum at $7.3 \cdot 10^{-4}\,\mathrm{s}^{-1}$ for the low wRHi, to a maximum at $8.2 \cdot 10^{-4}\,\mathrm{s}^{-1}$ for the medium wRHi, and to a maximum at $9.3 \cdot 10^{-4}\,\mathrm{s}^{-1}$ for the high wRHi~~ , as can be seen in both data sets, the high resolution radiosonde data (Fig. **??**), ~~respectively. We find for~~ and the ERA5 ~~values from $5.7 \cdot 10^{-4}\,\mathrm{s}^{-1}$ for the low wRHi category, to $6.5 \cdot 10^{-4}\,\mathrm{s}^{-1}$ for the medium wRHi category, and to $7.0 \cdot 10^{-4}\,\mathrm{s}^{-1}$ for the high wRHi category~~ data (Fig. **??**), respectively. The values of the maximum of the modes for the different categories is listed in Table **??**. It is important to mention that the PDF broadens with higher wRHi, which means that the variance of the sTIL values increases. The increased variance does not lead to the different PDF to cross in the left tail of the function, meaning that weak sTIL always have a higher probability to be in the lower humidity category. Similarly higher sTIL values (> ~~$9.3 \cdot 10^{-4}\,\mathrm{s}^{-1}$~~ $9.3 \times 10^{-4}\,\mathrm{s}^{-2}$ for radiosondes and > ~~$6.5 \cdot 10^{-4}\,\mathrm{s}^{-1}$~~ $6.5 \times 10^{-4}\,\mathrm{s}^{-2}$ for ERA5) have a higher probability of being part of the higher wRHi category.

When comparing the radiosondes (Fig. **??**) and ERA5 (Fig. **??**) the similar shape in the probability density and the same trends are apparent, while the values of sTIL are shifted to lower values when comparing ERA5 with the radiosondes.

Again we find the same qualitative behaviour for RS data and reanalysis data, although the quantitative values differ due to the different vertical resolution of the data. Overall, we can state that there is a strong indication that high RHi values are physically connected with strong TILs (via the relevant adiabatic and diabatic processes).

3.2.2 TIL depth and humidity

In addition to the strength of the TIL, ~~the depth of the TIL also shows a correlation with the RHi, which is discussed in this section.We show again pdfs~~ we show in Fig. **??** distributions of the TIL depths dTIL distributed into different classes of

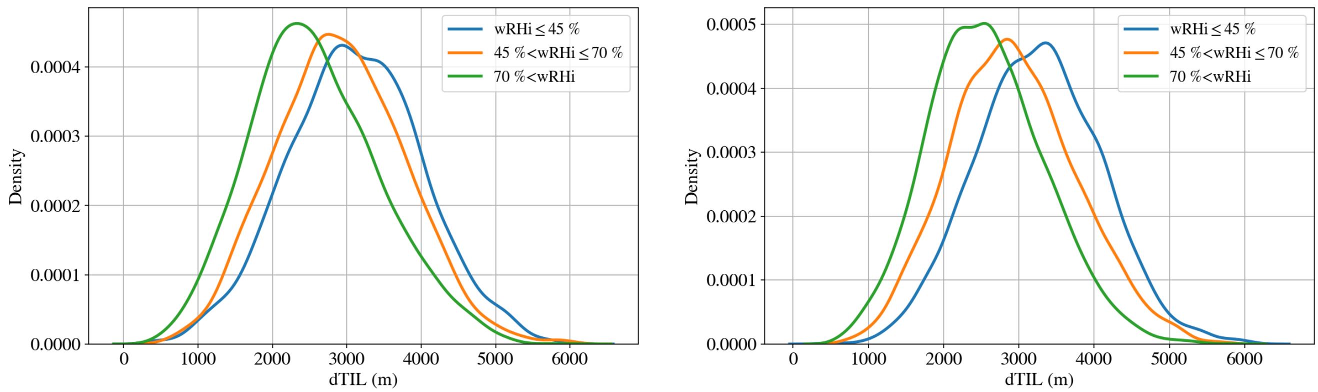

(a) Radiosondes

(b) ERA5

Figure 9. Probability density distribution for the radiosondes RSD (a) and ERA5 (b) of the tropopause inversion layer depth dTIL for categories of average relative humidity over ice wRHi. The low category (wRHi $\leq$ 45 %) in blue, the medium category (45 % < wRHi $\leq$ 70 %) in orange and the high category (70 % < wRHi) in green.

averaged relative humidity with respect to ice wRHi. Here, the depth of the TIL also shows a correlation with the RHi~~(Fig. ??). As the average relative humidity over ice wRHi increases, the TIL depth dTIL is shifted to lower values.~~ , which is discussed in this section. The total width of the distribution does not change, so the depth of the TIL is always in the range between some few hundreds metres up to about ~~6000 m.~~ 6000 m; however, the maximum of the distribution shows a clear deviation. As the average relative humidity over ice wRHi increases, the TIL depth dTIL is shifted to lower values.

The probability density function shows a formation of a second mode, as found in the ERA5 data set for all wRHi classes (Fig. **??**), as well as in the low wRHi category of the measurements (blue line, Fig. **??**). This formation of a double mode is an ~~artifact of the categorisation processand is thus~~ artefact of the categorization process, in which the aim was to ensure that one third of the data per category was included. These double modes are therefore not of a physical nature. The origin is a fluctuation in the distribution, which is cut off by the boundaries of the categorisation. The artifact makes the interpretation of the mode difficult. Nonetheless there is a clear correlation between higher dTIL values and lower wRHi values ~~and the~~ . The variance of the data within each wRHi category is about the same, seen by the similar width and height of the PDF.

Despite the different resolutions of the underlying data, the results between ERA5 and the radiosonde data are very similar. The maximum of the distributions for the high wRHi category is approximately 2250 m in both cases. In contrast, the thickness of the TIL in the driest category low wRHi is around 3000 m. The category in the middle with wRHI between 45 % and 70 % is about 2900 m in both data sets. As mentioned above, the double mode makes exact quantification difficult.

In summary, it can be seen that the drier the air is in this region, the thicker the TIL is. ~~Or in~~ In other words, a moist upper troposphere ~~is sharpening the TILin terms of their depth~~coincides with a decreased depth of the TIL. In combination with the findings from the section before, we can conclude, that for a more humid upper troposphere, we can ~~expect~~ find a stronger but vertically more confined TIL feature. This confinement might be driven by radiative processes, since a sharp moisture gradient at the tropopause level leads to a strong but vertically very confined radiative effect (see, e.g., figure 9 in **?**). In addition, a strong vertical upward motion as triggered by adiabatic processes might also lead to a confinement of the vertical TIL features. However, a clear attribution of this connection is not possible, although the enhanced humidity points again to the adiabatic and diabatic processes.

3.3 Geographical variations

We found a correlation between TIL characteristics and humidity for the Idar-Oberstein site in Central Europe with radiosonde measurements and reanalysis data; thus, the next step is to investigate three additional regions ~~in the northern hemisphere~~ representative for northern hemisphere extratropics at a similar latitude with different meteorological conditions but at different longitudes. Here, we address the question whether similar correlations can be found there, although the meteorological situation might be different in terms of large scale dynamics, i.e. in terms of developing baroclinic instabilities or evolving frontal systems. For this purpose, solely the reanalysis data are now used because of lack of high resolution radiosonde data with acceptable measurement quality for humidity variables.

Idar-Oberstein (Central Europe, C.E., 49.69°N and 7.33°E), which has already been highlighted in detail, has a low cyclone frequency with its maximum in the spring months MAM. The second location is in central Asia (C.A., 49.75°N and 87.25°E) with almost no cyclonic activity throughout the year. The third location is in central USA (USA, 42.50°N and -86.5°E), where the cyclonic frequency for the region is high in winter DJF and spring MAM, and low in summer JJA and autumn SON. The fourth location is in the North Pacific N.P. (49.75°N and -172.75°E), with very high cyclonic frequency through out the year except for a strong minimum in summer (**?**).

As already investigated for the Central Europe region (Figure **??**), the TIL strength is also distributed into the different moisture classes for the other locations. The results are presented in Figure **??** and confirm that the sTIL values tend to be higher when the average relative humidity with respect to ice is also high for the other regions. Also, the variability of sTIL is increasing with increased humidity in all regions. However, it is visible that the different regions exhibit different distribution shapes of the TIL strength. For example the central USA is showing the highest variability of the sTIL and the highest probability of strong sTIL events. On the contrary central Asia is showing the lowest variability and the lowest probability of strong sTIL events.

To summarize, ~~it can be stated that the influence of humidity on the strength of the TIL~~ the co-occurrence of high values of humidity with strong values for sTIL is a robust feature of the extratropics.

The higher the averaged humidity is, the stronger is the resulting TIL.

3.4 Seasonal variations

This section ~~is covering~~ deals with the seasonal variation of the tropopause inversion layer, which is also ~~covered by the literature, finding that the effect of water vapour~~ discussed in the literature. It was found that the interplay of water vapor on the static stability in the UTLS region ~~to act~~ occurs on seasonal time scales (**??**).

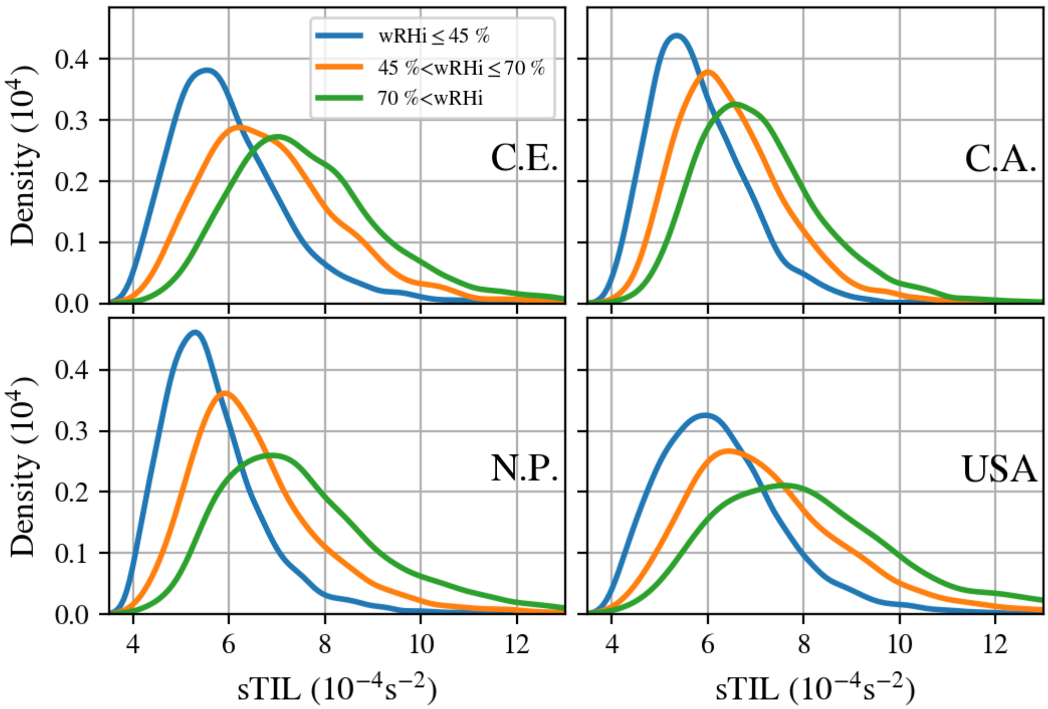

Figure 10. The probability density function of the TIL strength sTIL for average relative humidity categories. Central Europe C.E. (upper left), central Asia C.A. (upper right), the Northern Pacific N.P. (lower left) and the central USA (lower right).

3.4.1 Seasonal mean vertical profiles

Starting with the temperature profile for central Europe (Fig. **??**) the highest temperatures in the stratosphere and troposphere are found in the summer months; similarly the lowest temperatures are found in the winter months. The autumn and spring months show similar temperatures in the troposphere and at tropopause level, but significantly differ in the stratosphere with autumn temperatures being colder than spring temperatures. For higher levels, the autumn temperatures match the winter temperatures.

The averaged RHi for central Europe on average show little seasonal difference in the troposphere. The most pronounced seasonal differences are found in the first kilometer above the tropopause. Based on the previous findings in section **??**, it is expected that the spring and summer months show the strongest TIL (high sTIL values) and the thinnest TIL (low dTIL values).

The static stability profiles show a peak of high static stability above the tropopause of similar magnitude ~~$N^2 = 6 \cdot 10^{-4}\,\mathrm{s}^{-1}$~~$N^2 = 6 \times 10$ across every season, with a significant difference in static stability above ~~the peak between seasons~~. Within the first 3 km above

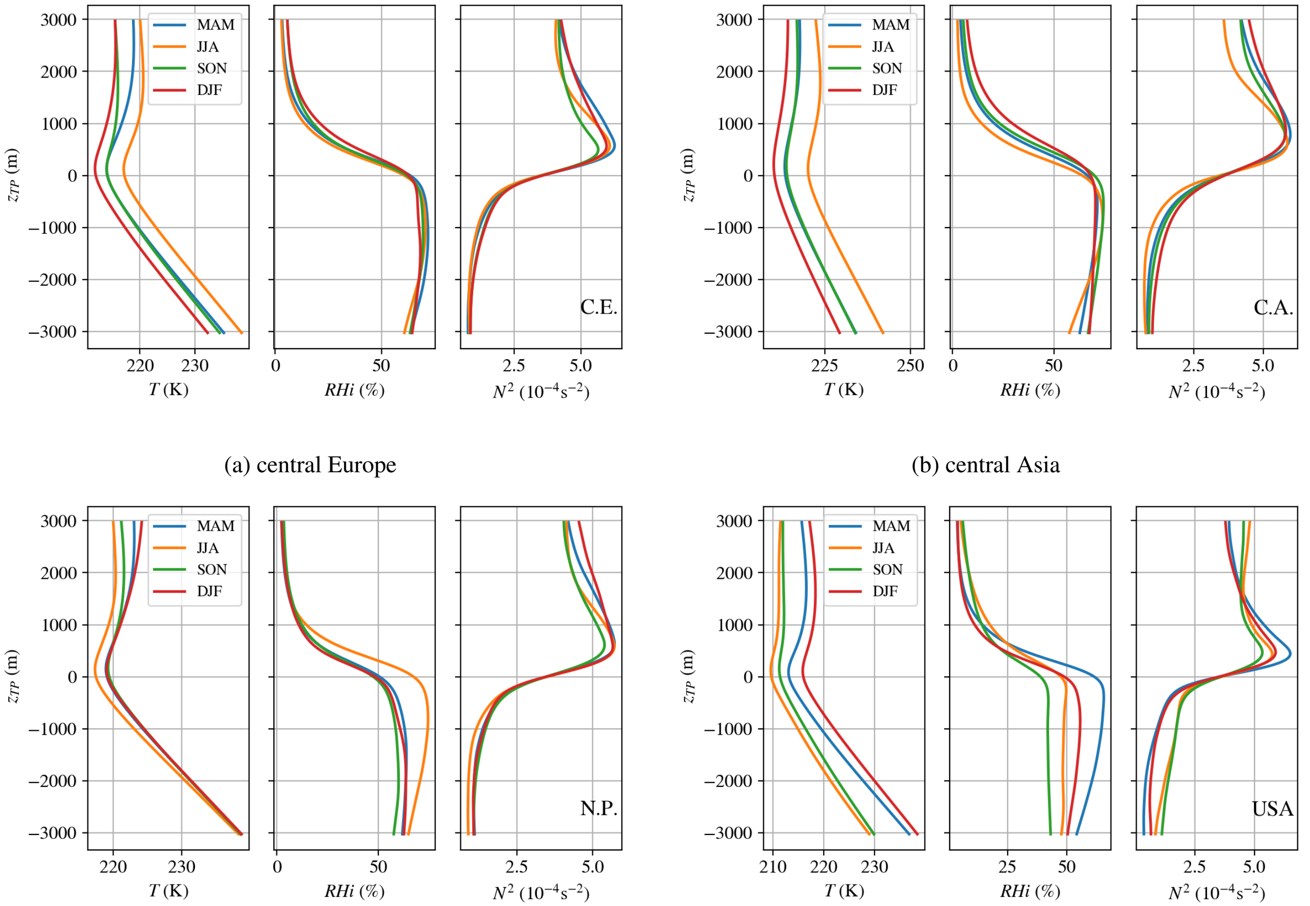

(a) central Europe

(b) central Asia

(c) Northern Pacific

(d) central USA

Figure 11. Mean vertical profiles of temperature T, relative humidity over ice RHi and static stability N^2 in the tropopause relative height z_{TP}. Colors indicate the different seasons, i.e., spring months (MAM) in blue, summer months (JJA) in orange, autumn months (SON) in green, and winter months (DJF) in red.

the tropopause the static stability is on average $0.48 \times 10^{-4}\,\mathrm{s}^{-1}$ in spring compared to autumn and $0.22 \times 10^{-4}\,\mathrm{s}^{-1}$ higher in winter compared to summer, confirming previous findings by **?** for the extratropic region (40 °N - 60 °N).

The vertical profiles over central Asia (C.A.) (Fig. **??**) show weak seasonal differences for RHi and the static stability. The summer and autumn months show slightly higher RHi below the tropopause. In contrast the temperature profiles show a high variability throughout the year with the highest temperatures in summer, the lowest temperature in winter.

The Northern Pacific region shows small or even no differences in the temperature and RHi profiles between spring, autumn and winter (Fig. **??**). However, the summer ~~seasonis~~ season is clearly different, the temperature profile is significantly colder in the tropopause region. At the same time, there is a strong increase in RHi above ~~2 km below the~~ the first km above the tropopause. This is supporting the idea that water vapour in the UTLS region has a cooling effect on the tropopause region (**??**). The static stability profile shows little seasonal differences, only the autumn months have a smaller static stability peak.

The central USA region shows the strongest seasonal differences in RHi and N^2. The RHi at the tropopause level takes on the highest values in spring followed by winter, summer and autumn in decreasing order. The peaks of N^2 show the similar pattern with spring exhibiting the strongest peak followed by winter, summer and autumn, respectively. The temperature profile is also different compared to the other regions, with summer exhibiting the lowest and winter the highest temperatures relative to the tropopause. ~~The stronger seasonal differences could be due to lower latitude (42.25 °N instead of 49.75 °N) which was performed~~ By design the central USA location was introduced to include a region of frequent deep convection in the extratropics. There, significantly higher CAPE values are present in the summer months compared to the other regions (**?**), indicating greater deep convection activity. This leads to a stronger seasonal cycle in the vertical profiles in this region.

3.4.2 Seasonal cycle of TIL strength

The correlation between TIL strength and relative humidity is split seasonally using the PDF for different moisture classes for all four regions. The same moisture classes using the average relative humidity with respect to ice (wRHi) as in Fig. **??** are used. The correlation of higher TIL strength (sTIL) values with higher averaged values of wRHi is consistent across every season and every geographical location. Furthermore the correlation of higher sTIL variances with higher wRHi is also present in every region. Also, a distinct feature independent of the geographical region or season is that the low wRHi category shows a mode between ~~$5\cdot10^{-4}\,\mathrm{s}^{-1}$~~$5\times10^{-4}\,\mathrm{s}^{-1}$ and ~~$6\cdot10^{-4}\,\mathrm{s}^{-1}$~~$6\times10^{-4}\,\mathrm{s}^{-1}$ with a very low occurrence probability above ~~$8\cdot10^{-4}\,\mathrm{s}^{-1}$~~$8\times10^{-4}\,\mathrm{s}^{-1}$.

The region over Central Europe and Central USA show a similar seasonal behaviour. The highest values of sTIL (i.e. "strongest TIL") are found in the spring months, while the minima are found in autumn. The winter months show higher variance and stronger extremes compared to summer, which show on average similar sTIL values as in winter. The winter/summer similarity further support the idea ~~that radiative and baroclinic forcing~~ (according to **?**) that adiabatic processes (i.e. baroclinic forcings) and diabatic processes (e.g. radiative or latent heating) can have similar amplifying effects~~. The~~, although the time scales might not necessarily be the same. The evolution of baroclinic instabilities takes place within days, whereas radiative processes might act on time scales up to few days (if the water vapor concentration is not changed drastically in between). However, cloud processes might act on much shorter scales (minutes to hours). Thus, a clear attribution remains difficult or even impossible. The main difference between central Europe and USA is the considerably higher variance of sTIL in the USA region. Looking at the cyclonic frequencies, the USA region shows a higher frequency than the central Europe across every season. Higher frequency alone does not explain the high variance as the North Pacific with the highest cyclonic frequency do not show higher variance in sTIL. This needs further research in the causes and the forcing mechanisms of the tropopause inversion layer.

The lowest variance of sTIL are found in central Asia (Fig. **??**) across each season and humidity category. **?** suggested a strengthening of the TIL by baroclinic waves. The baroclinic waves are rare in central Asia as deduced from the low cyclonic frequency, which could explain weaker sTIL values ~~compered~~ compared to the other region, where baroclinic waves occur

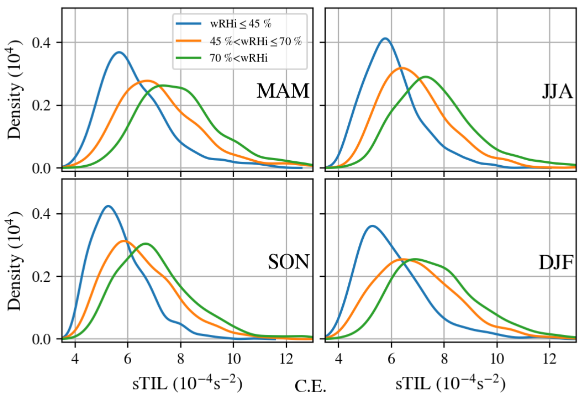

(a) Central Europe

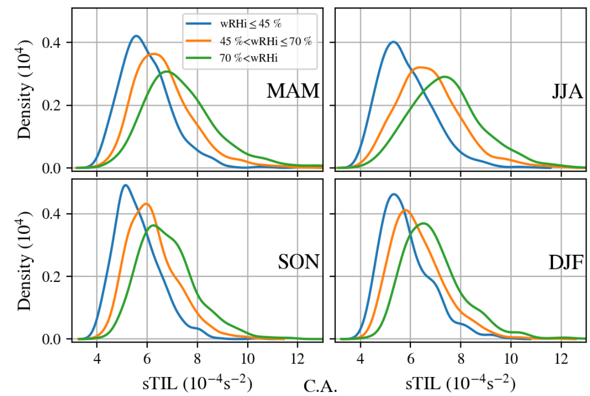

(b) Central Asia

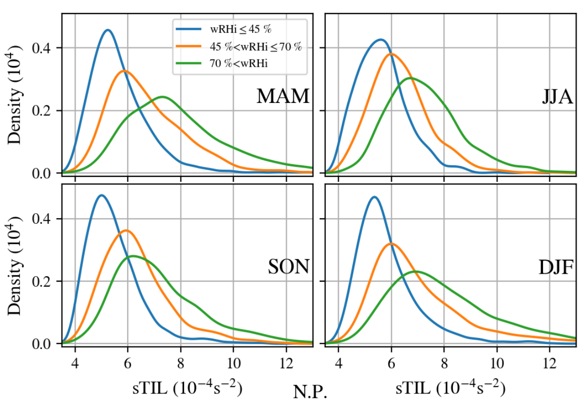

(c) Northern Pacific

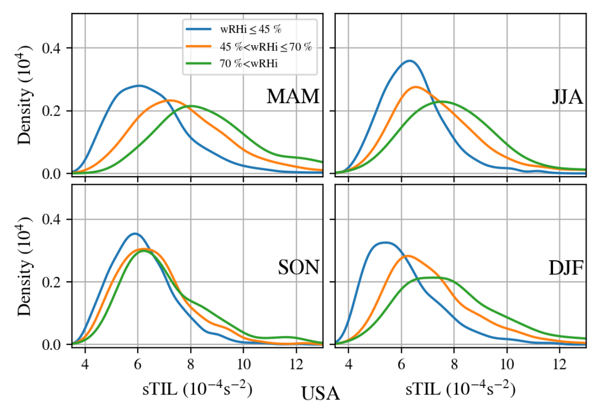

(d) Central USA

Figure 12. Seasonal probability density distributions of the tropopause inversion layer strength sTIL for categories of average relative humidity over ice wRHi. Colors indicate the different categories. blue: low category (wRHi $\leq$ 45 %), orange: tmedium category (45 % < wRHi $\leq$ 70 %), green: high category (70 % < wRHi). The panels represent the behaviour for different resions, i.e., results for Central Europe are shown in (a), for Central Asia in (b), Northern Pacific in (c) and Central USA in (d). In addition, in each subfigure the season is indicated, i.e., spring months (MAM), summer months (JJA), autumn months (SON), and winter months (DJF).

more frequently. Also, in Central Asia the highest sTIL values are found in the summer months, which is more characteristic of the polar TIL as demonstrated by **?** and **?**. This maximum in sTIL in summer observation supports the radiative mechanism suggested by **?**, since the forcing mechanism by baroclinic waves is reduced to a minimum for this region

The region over the Northern Pacific (Fig. **??**) shows a maximum of sTIL values in the winter and spring months, and a similar minimum in autumn and summer. The maxima are most likely due the baroclinic wave activity, which has its maximum in spring and winter. It is noticeable that the mode in the wettest wRHi category is at higher sTIL values in spring than in winter. This is suggesting that water vapour and its radiative forcing is amplifying the sTIL in spring. The comparison between autumn and summer also shows an interesting aspect. The cyclonic activity has a significant minimum in summer and is lower in autumn than in spring and winter, nonetheless spring and summer are exhibiting similar sTIL values. This gives the indication that the forcing mechanism through baroclinic waves and through the radiative effects might have a similar amplitude, but may act on different time scales.

~~Overall~~Altogether, consideration of seasonal and geographic differences reveals the overall robust relationship between the strength of TIL and ~~mean moisture~~ average humidity with respect to ice in the upper troposphere (wRHi). However, if one looks more closely at the seasonal cycle in different regions with different synoptic characteristics, one finds different processes seen over the year. At the same time evidence for different formation mechanisms for TIL (radiative forcing, baroclinic waves) can be found.

4 Conclusions

~~Here we investigated the relationship between various properties of the TIL and relative humidity in the upper troposphere. The example of the long-term series of radiosonde measurements at the Idar-Oberstein station of the German Weather Service clearly showed that the strength of the TIL is strongly related to the relative humidity in the upper troposphere. This can be seen not only in the spatially high-resolution measurement data, but also in the reanalysis data from ERA5 at the same location. The interpolated values reflect the radiosonde's perspective very well, with the expected reductions in the signal due to the coarser spatial resolution of the reanalysis data, such as the weaker representation of gradients in ERA5.~~

~~The comparison of the meteorological variables temperature T,~~ From theory and former model investigations we can assume that the variable relative humidity over ice is a very meaningful quantity for the investigations of properties of the tropopause inversion layer. Since the formation and sharpening is first driven by adiabatic compression of the isentropes and afterwards enhanced by irreversible diabatic processes, high values of relative humidity over ice ~~RHi and static stability N^2 showed that the average difference of a single profile between~~ are important marker for both occurring processes. For a detailed investigation we used high resolution radiosonde data over one German site (Idar-Oberstein, 49.69° N, 7.33° E) and the ERA5 ~~and radiosondes are small. In more detail it was found that the reanalysis data shows on average slightly warmer temperatures in the upper troposphere (0.034 K~~data from the reanalysis project of the ECMWF (ERA5 grid point at 49.75° N, 7.25° E). In ~~the lower stratosphere this deviation is slightly higher (0.121 K). Nevertheless, the comparison shows that the reanalysis data can be used for this kind of investigations very well . Regarding the relative humidity, one can see that the model data is slightly moister (approx. 1.2 % RHi) compared to~~ a first step, we could show that both data agree very well and are both able to represent the TIL and its features quantitatively and qualitatively. In a second step, the properties of the ~~radiosondes. The static stability profiles show a too stable behaviour in the UT and a too unstable behaviour in the LS. This difference arises through the coarser resolution of ERA5 which leads to lower absolute values in static stability and weaker gradients in static stability when compared to the radiosondes.~~

~~The TIL strength sTIL is considerably weaker in ERA5 then in the radiosonde data, also the variance increases with stronger sTIL. It shows a strong linear correlation, which makes the sTIL a good measure of the tropopause inversion layer to compare across reanalysis and measurement data.~~

~~It could be shown that there is a strong positive correlation between the TIL strength sTIL and the average relative humidity with respect to ice wRHi, meaning that higher sTIL are correlated with higher wRHi. It also could be shown that the variance of sTIL increases with higher wRHi. These findings are found in~~ TIL in comparison with some mean relative humidity measure are investigated. As a major result, we find that sharper or stronger TILs occur for higher RHi values, which points to the adiabatic contribution (i.e. adiabatic lifting of the moist layers), and also for sharper gradients of RHi at the moist layer's top, which points to the diabatic processes (e.g. radiative effects). These result are very robust through seasonal variations, as obtained from further analysis of the ERA5 ~~and in the radiosondes dataset. Additionally, the TIL depth dTIL shows a negative correlation with wRHi, meaning that that thinner TILs are correlated with higher wRHi~~data.

~~Extending the analysis with ERA5 to other geographical regions at approximately the same latitude (between 42° and 50° N,~~ In addition, the connection between high humidity values and strong TILs can be found at other extratropical geographical regions, namely Central USA, Central Asia and Northern Pacific ~~) showed that the overall correlation are independent of the region and season. The regional and seasonal analysis also allowed to confirm that the two suggested forcing mechanisms, the dynamical forcing by ? and~~ at approximately the same latitude througout all seasons. Again, variations in the strength and moisture values might be related to differently strong activity in large scale flows, i.e. in baroclinic instabilities and frontal systems.

Overall, we can state that the ERA5 data is well suited for this kind of investigations, the qualitative features of TILs are well represented. The connection between relative humidity and TIL features is robust and corroborates the former findings in model studies by **?**. Although it is not possible to discriminate the adiabatic and diabatic components in the analysis, we could show that the relative humidity is well suited for this kind of analysis, pointing to the relevant processes for the evolution of the ~~radiative forcing by ? are present. For central Europe, the central USA and the Northern Pacific, sTIL showed is maximum in the seasons of highest cyclonic frequency, this is supporting the dynamical forcing. Central Asia, which is unaffected by cyclonic activity, shows its maximum of sTIL in summer and its minimum in winter and thus supporting the radiative forcing mechanism~~tropopause inversion layer.

Code availability. Code for the data processing and analysis is provided on Zenodo (https://zenodo.org/records/10604349).

Data availability. The radiosonde data are publicly available from https://opendata.dwd.de/ at DWD. The ERA5 reanalysis data are publicly available from https://cds.climate.copernicus.eu at ECMWF

Author contributions. DK, PR and PS designed the study; DK carried out the data analyses; DK, PR, and PS contributed to interpreting the results and writing the paper.

Competing interests. The contact author has declared that none of the authors has any competing interests.

Disclaimer. Publisher's note: Copernicus Publications remains neutral with regard to jurisdictional claims in published maps and institutional affiliations.

Acknowledgements. We thank Deutscher Wetterdienst (DWD) for providing the high resolution radiosonde data, and the European Centre for Medium-Range Weather ~~Forecasting~~ Forecasts (ECMWF) for providing the ERA5 reanalysis data. We thank Daniel Kunkel for fruitful discussions, and for getting the data from ECMWF. We also thank Peter Hoor for fruitful discussions. Philipp Reutter acknowledges support by the DFG within the Transregional Collaborative Research Centre TRR301 TPChange, Project-ID 428312742 , project C1. Peter Spichtinger acknowledges support by the DFG within the Transregional Collaborative Research Centre TRR301 TPChange, Project-ID 428312742, project B7. The study contributes to the project "Big Data in Atmospheric Physics (BINARY)", funded by the Carl Zeiss Foundation (grant P2018-02-003). The authors thank the two anonymous reviewers for their constructive comments and suggestions that improved the paper.